Cell Reports, Volume *25*

Supplemental Information

RBM17 Interacts with U2SURP and CHERP to Regulate Expression and Splicing of RNA-Processing Proteins

Antonia De Maio, Hari Krishna Yalamanchili, Carolyn J. Adamski, Vincenzo A. Gennarino, Zhandong Liu, Jun Qin, Sung Y. Jung, Ronald Richman, Harry Orr, and Huda Y. Zoghbi

SUPPLEMENTAL FIGURES TITLES AND LEGENDS

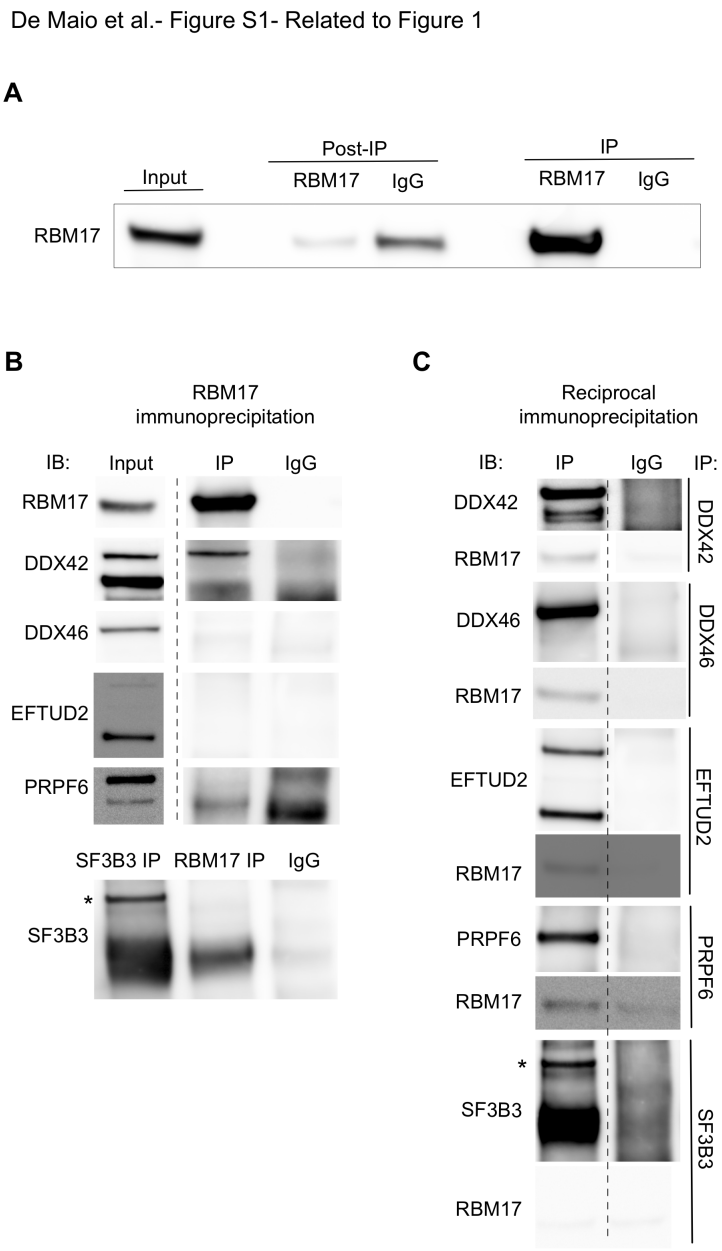

Figure S1-Related to Figure 1. Immunoprecipitation and mass spectrometry identify RBM17 protein interactors. (A) Example of RBM17 immunoprecipitation from 12-week-old wild-type mouse cerebellum in the conditions used for IP-MS. (B) Representative western blot showing results for the immunoblot analysis of input, RBM17 IP and IgG samples for the proteins considered weak interactors (DDX42, DDX46, EFTUD2) or not interacting with RBM17 (PRPF6, SF3B3) among those in Fig. 1B. * indicates the band of the proper molecular weight for SF3B3 (C) Reciprocal IP of the protein not interacting or weakly binding RBM17 to confirm results of the RBM17 direct IP. The presence of a dashed line indicates that the image of the membrane has been modified to remove lanes irrelevant to the results.

De Maio et al.-Figure S2-Related to Figure 2

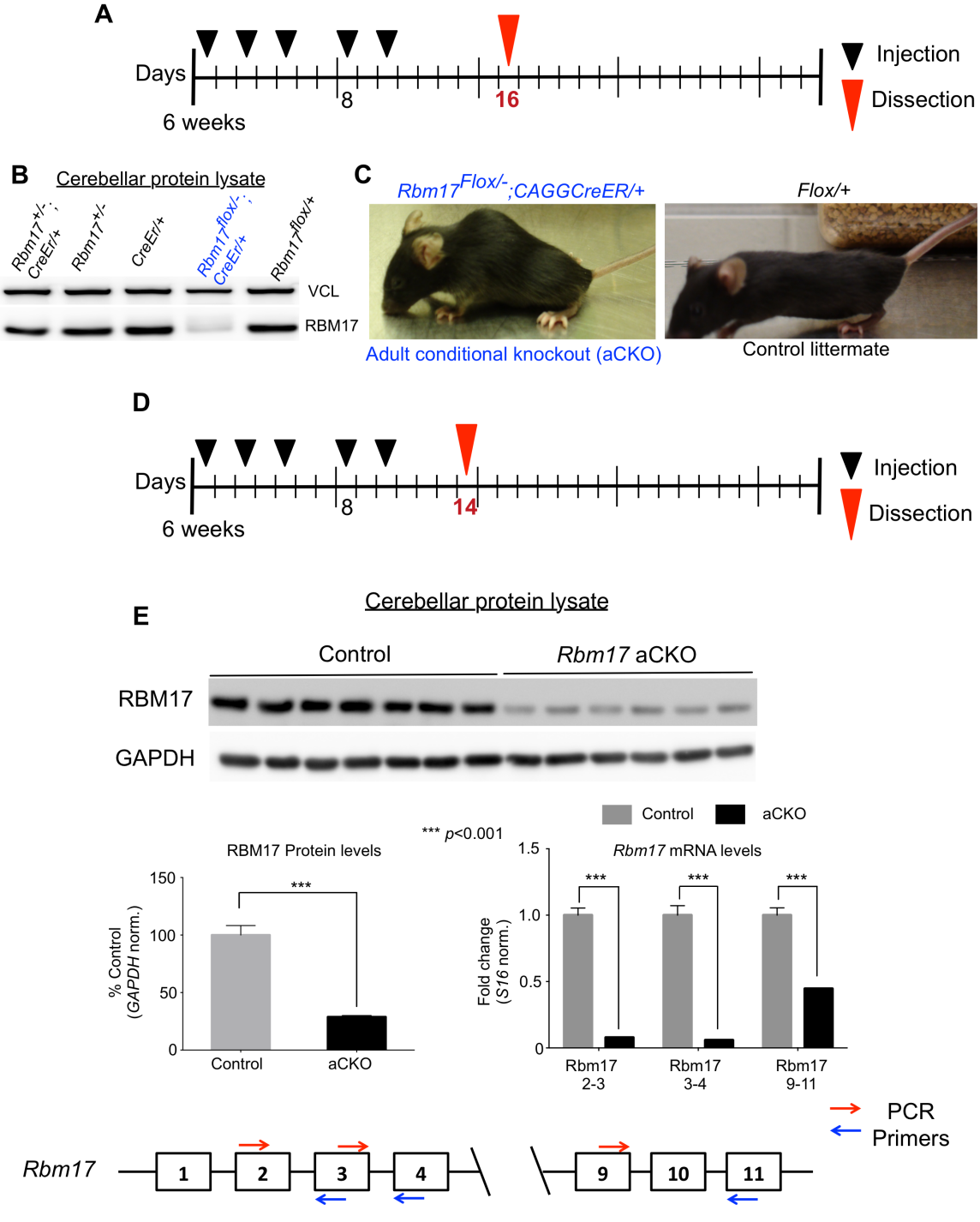

Figure S2-Related to Figure 2. Deletion of *Rbm17* in adult mice is lethal. (A) Schematic representation of the tamoxifen administration paradigm to generate *Rbm17* adult conditional knockout mice (aCKO). (B) Representative western blot analysis of cerebellar protein lysate from one cohort of mice treated as indicated in Figure S2A (n = 1/genotype). (C) On the left, appearance of an aCKO mouse at day 16 after the first injection, and on the right a control littermate treated with the same tamoxifen regimen. (D) Schematic representation of the modified tamoxifen administration paradigm to obtain healthier aCKO. (E) Quantification of protein and RNA levels in cerebellar samples from aCKO mice treated with tamoxifen as by paradigm in S2D; n = 6 aCKOs and n = 7 control littermates. Data represent mean ± SEM; p value was calculated by two-tailed Student's t test and significance was set at $p< 0.05$. The schematic represents the position of the three different set of primers (Rbm17 2-3, Rbm17 3-4, Rbm17 9-11) used to quantify *Rbm17* mRNA by qRT-PCR.

De Maio et al.- Figure S3- Related to Figure 3

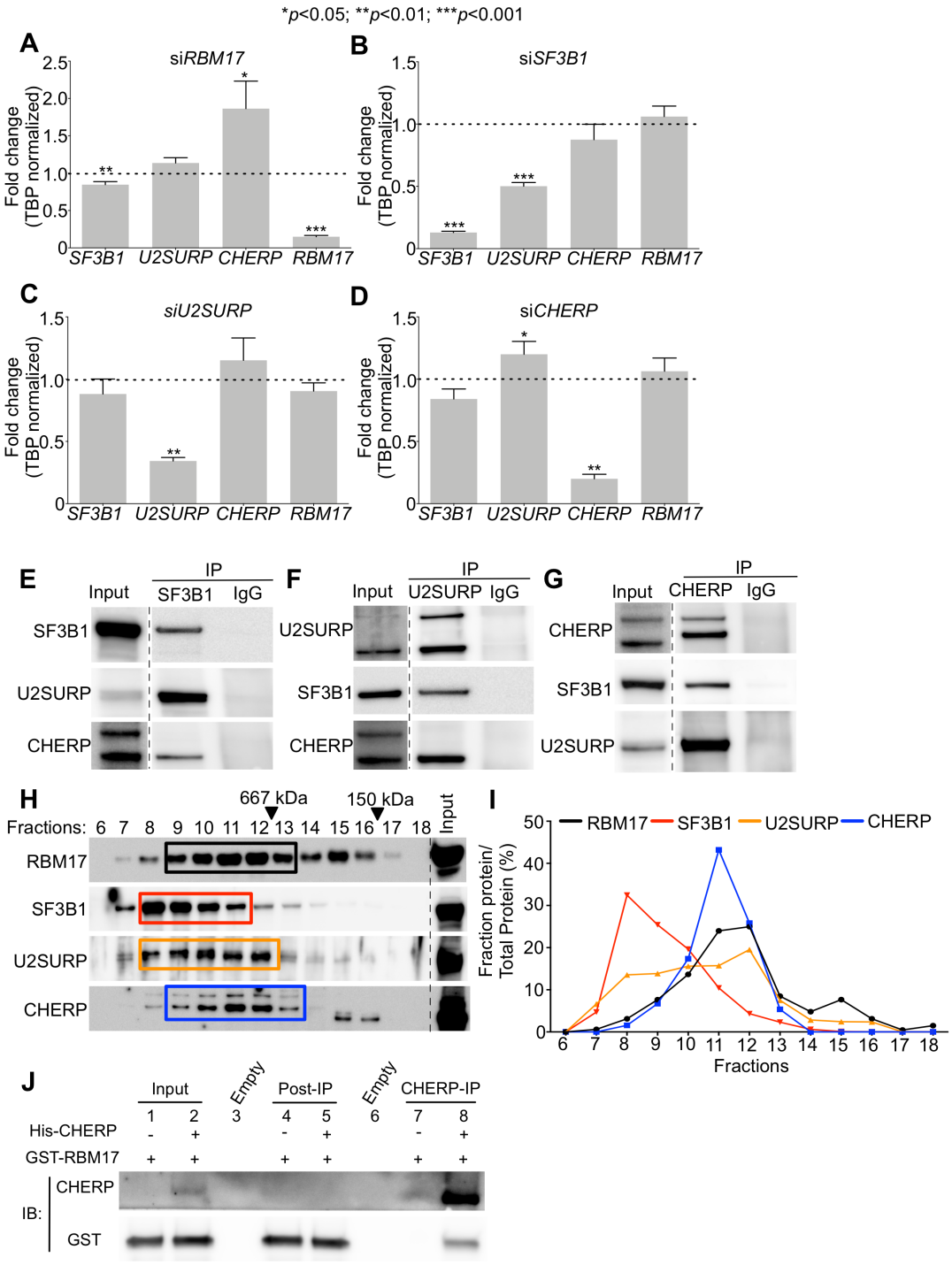

Figure S3-Related to Figure 3. RBM17, SF3B1, U2SURP, and CHERP interact with each other and regulate reciprocal protein stability. Levels of *RBM17, SF3B1, U2SURP, CHERP* mRNA were measured using qRT-PCR on samples from HEK293T cells treated with (A) *siRBM17*, (B) *siSF3B1*, (C) *siU2SURP* or (D) *siCHERP* and compared to cells treated with *siScramble*; n = 9-18 replicates/siRNA and bars represent mean ± SEM; p value was calculated by two-tailed Student's t test and significance was set at $p< 0.05$. (E-G) Western blot analysis of the *in viv*o IPs of (E) SF3B1, (F) U2SURP or (G) CHERP from 12-week-old wild-type mouse cerebellum along with IgG controls; each western blot has been immunolabeled for the three interacting proteins, showing that the immunoprecipitated target protein pulls down the other two factors. (H) Fractionation pattern of wild-type mouse brain lysates analysed by western blot and immunolabeled for RBM17, SF3B1, U2SURP and CHERP. (I) Quantification of the percentage of protein per fraction over the total amount of the same protein contained in the fractions between 6 and 18. (J) Representative western blot analysis of the *in vitro* co-immunoprecipitation of recombinant CHERP and GST-RBM17 run in two independent replicates. The membrane was probed for CHERP and GST to detected GST tagged RBM17. Lanes labelled empty contain no sample and were skipped to avoid contamination. The presence of a dashed line indicates that the image of the membrane as been modified to remove lanes irrelevant to the results.

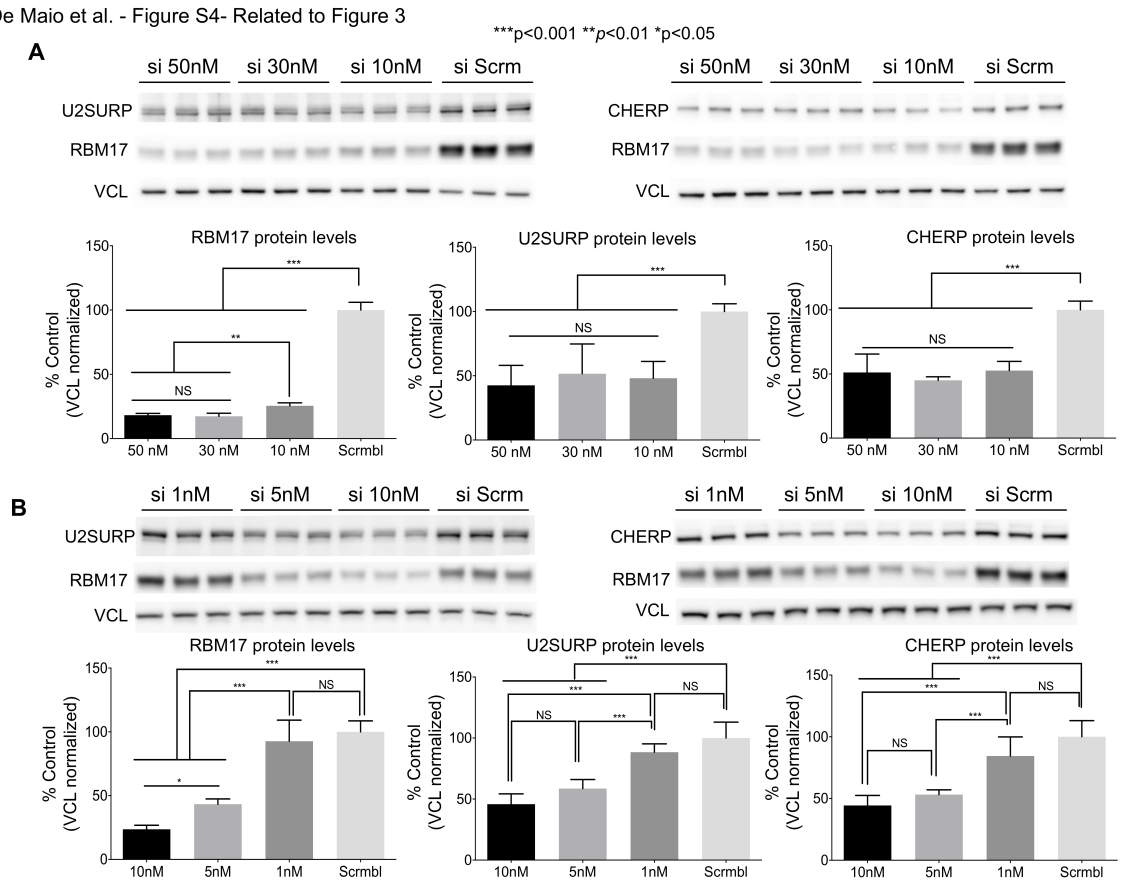

Figure S4-Related to Figure 3. The levels of U2SURP and CHERP correlate in a dose-dependent way with the levels of RBM17. Representative western blots and protein level quantification for U2SURP and CHERP upon knockdown of *RBM17* using (A), 50nM, 30nM or 10nM or (B) 10nM, 5nM or 1nM of *siRBM17*. Cells were treated with Scramble siRNA as control (si Scrm). All data were normalized to VCL, used here as loading control. n = 6 replicates/siRNA and the bars in each quantification graph represent mean ± SEM; p value was calculated using GraphPad-Prism by one-way ANOVA followed by Tukey's multiple comparisons test and significance was set at $p < 0.05$.

De Maio et al. - Figure S5- Related to Figure 6

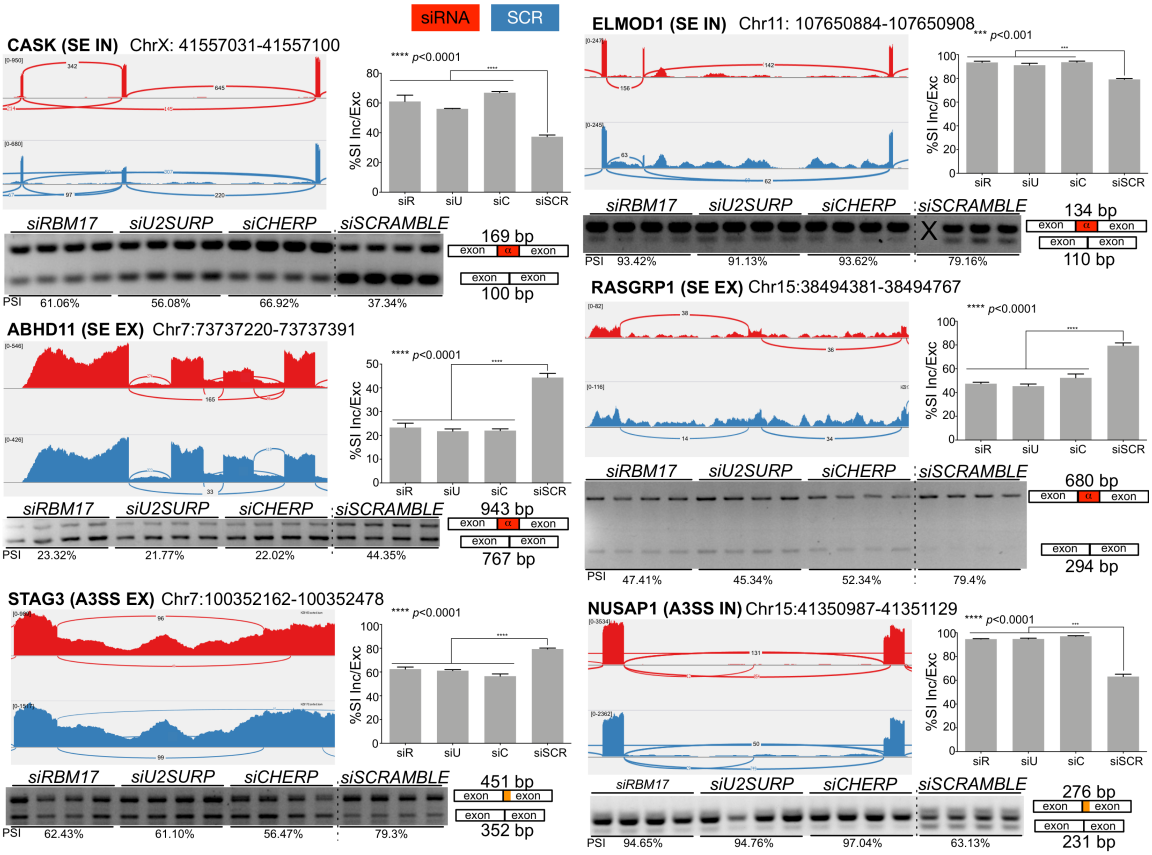

Figure S5-Related to Figure 6. Validation of selected splicing alterations identified by rMATS. Selected aberrant splicing events were validated using RT-PCR on samples from HEK293T cells treated with *siRBM17* (siR), *siU2SURP* (siU) or *siCHERP* (siC) and compared to cells treated with siScramble (siSCR) (n = 4 replicates/siRNA). For each event are depicted: 1) the sashimi plot, representing the actual sequencing trace at the specific genomic location, and the strength of the splicing junction in siRNA versus Scramble treated samples; siRNA-treated cells are represented by the red trace and siScramble-treated cells by the blue trace; 2) identification and separation of the different isoforms on agarose gel; 3) the quantification of the Percentage Spliced In (PSI) (see STAR Methods), where the bars represent mean ± SEM; p value was calculated by one-way ANOVA followed by Tukey's multiple comparisons test and significance was set at $p < 0.05$. The X on the gel image relative to the ELMOD1 gene indicates an empty well. Treatment and control samples are demarcated on the gel image by a dashed line.

De Maio et al. - Figure S6 - Related to Figure 6

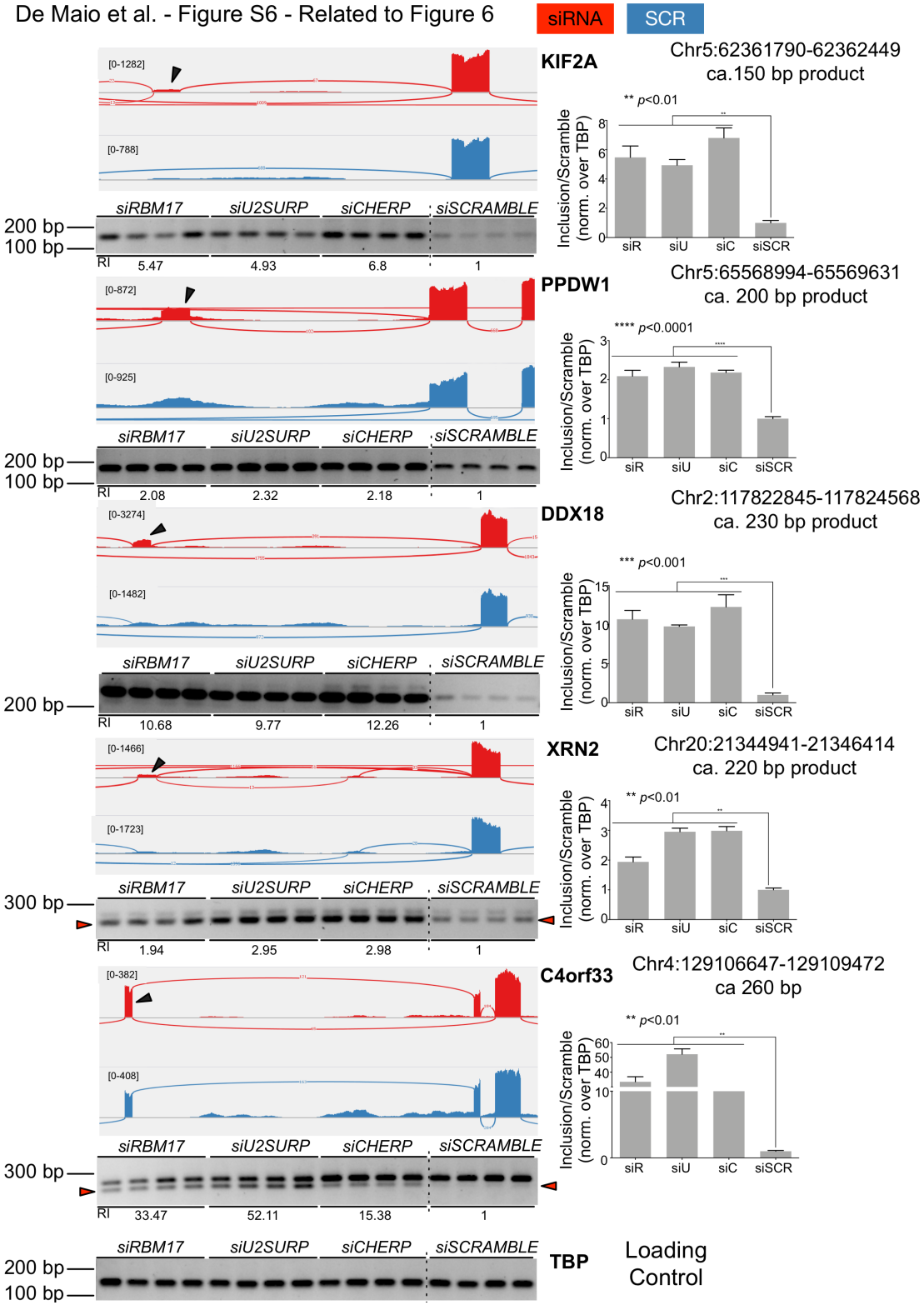

Figure S6-Related to Figure 6. Validation of selected cryptic splicing events identified by CrypSplice. Selected cryptic splicing events were validated using RT-PCR on samples from HEK293T cells treated with *siRBM17* (siR), *siU2SURP* (siU) or *siCHERP* (siC) and compared to cells treated with siScramble (siSCR) (n = 4 replicates/siRNA). For each event are depicted: 1) the sashimi plot, representing the actual sequencing trace at the specific genomic location and the strength of the splicing junction in siRNA versus Scramble treated cells; siRNA-treated cells are represented by the red trace and siScramble-treated cells by the blue trace; 2) the identification and separation of the different isoforms on agarose gel; 3) the quantification of the Relative Inclusion (RI) in siRNA versus Scramble treated samples (see STAR Methods); bars represent mean ± SEM; p value was calculated by one-way ANOVA followed by Tukey's multiple comparisons test and significance was set at $p< 0.05$. Black arrowheads point to the exon where the cryptic junction originates. Where present red arrowheads point to the quantified, correct band. Treatment and control samples are demarcated on the gel image by a dashed line.

De Maio et al. - Figure S7 - Related to Figure 6

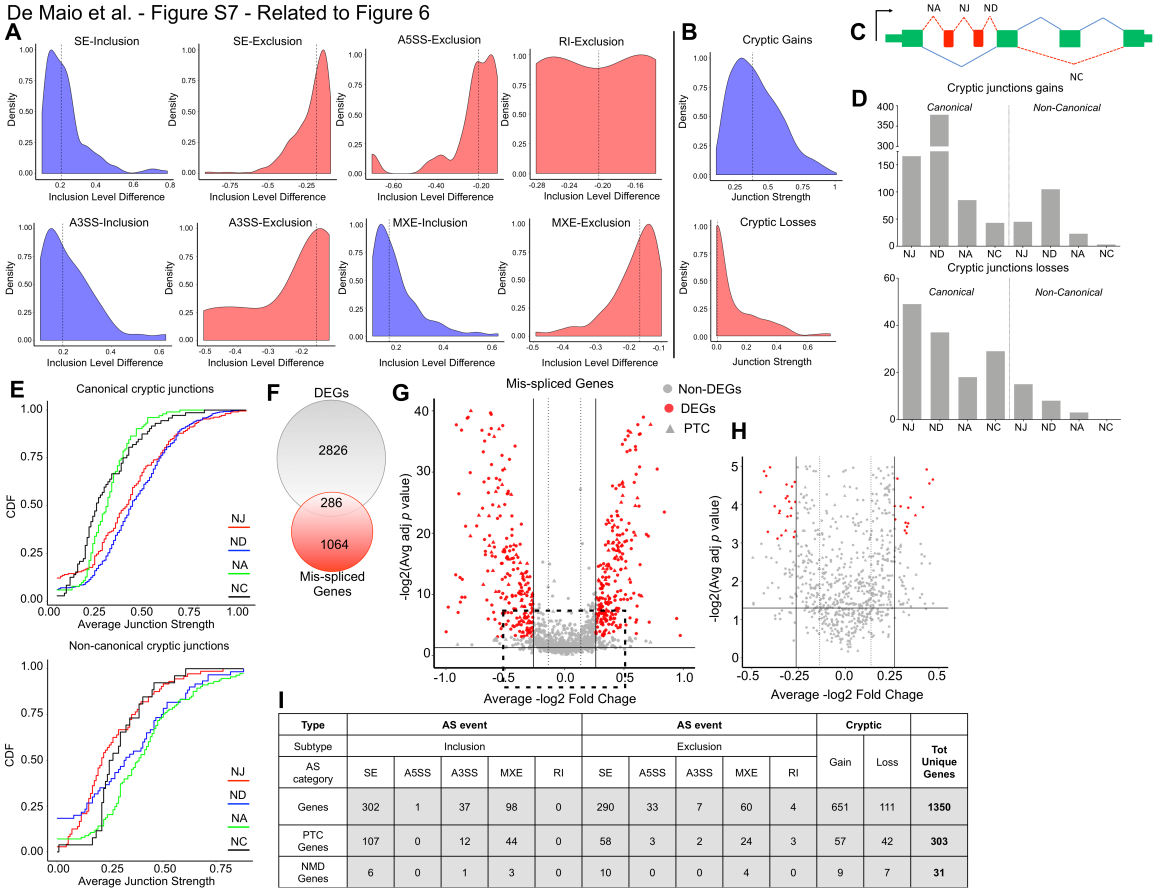

I

Type	AS event					AS event					Cryptic		
Subtype	Inclusion					Exclusion					Gain	Loss	Tot Unique Genes
AS category	SE	A5SS	A3SS	MXE	RI	SE	A5SS	A3SS	MXE	RI			
Genes	302	1	37	98	0	290	33	7	60	4	651	111	**1350**
PTC Genes	107	0	12	44	0	58	3	2	24	3	57	42	**303**
NMD Genes	6	0	1	3	0	10	0	0	4	0	9	7	**31**

Figure S7-Related to Figure 6. Characterization of the splicing changes shared upon knockdown of *RBM17*, *U2SURP* or *CHERP*. (A) Plots of density over mean inclusion level difference of the splicing changes detected by rMATS and common among the knockdown of RBM17, U2SURP and CHERP. (B) Plots of density over mean junction strength of the splicing changes detected by CrypticSplice and common among the knockdown of RBM17, U2SURP and CHERP. (C) Schematic representing the classes of cryptic splicing events that upgraded CrypSplice can distinguish: Novel Junction, NJ; Novel Donor, ND; Novel Acceptor, NA; Novel Combination, NC. (D) Absolute count of cryptic events per sub-category. (E) Analysis of the cumulative distribution function (CDF) of the subcategories of cryptic splicing events identified by CrypSplice and further distinguished in canonical and non-canonical events according to sequences at the splice sites marking the junctions (being them the consensus GU-AG di-nucleotides or different short sequences). (F) Venn diagram indicating the absolute number of genes commonly altered in the three knockdowns and harboring gene expression changes only, splicing changes only or both. (G) Scatter plot of mean log fold change to mean -log adjusted p-values of differentially splice genes. Transcripts that are also differentially expressed more than 20% compared to control, in all the three knockdown samples, are in red. PTC harboring genes are marked as triangles. (H) Zoom in of the portion of the Volcano plot in (G) enclosed within a dashed box. This section highlights the presence of mis-spliced genes whose transcripts show no gene expression change or a differential expression that does not meet the 20% cutoff (solid black vertical line). (I) Number of genes that harbor splicing alterations inducing Premature Termination Codons (PTCs) and of the portion of such genes that also exhibit down-regulation as a putative consequence of Nonsense Mediated Decay (NMD). The Total number of unique genes in the last column does not intend to be the sum of the numbers indicated in each of the preceding columns. It is instead the final count of putative NMD-genes irrespectively of the number of aberrant splicing events each of these genes carries (See also STAR Methods).

Table S5-Related to Figure 6. Detailed analysis of the shared alternative splicing changes caused by knockdown of *RBM17*, *U2SURP* or *CHERP*. Percentages are calculated over the smallest and the largest of the three datasets. Columns titles are bold. Abbreviations are explained in Figure 6.

Splicing category	***siRBM17***		***siU2SURP***		***siCHERP***		**Overlap**	
	Total		**Total**		**Total**		**Total**	
	Exc	Inc	Exc	Inc	Exc	Inc	**Exc**	**Inc**
SE	2566		2512		3589		**708 (19.8-28.18%)**	
	1374	1192	1347	1165	2201	1388	**347 (15.8-25.8%)**	**361 (26-31%)**
A5SS	123		140		143		**35 (24.5-28.5%)**	
	86	37	115	25	126	17	**34 (27-39.5%)**	**1 (2.7-5.9%)**
A3SS	201		194		242		**50 (20.7-25.8%)**	
	82	119	85	109	66	176	**7 (8.2-10.6%)**	**43 (24.4-39.4%)**
MXE	963		865		1522		**190 (12.5-22%)**	
	387	576	385	480	691	831	**72 (10.4-18.7%)**	**118 (14.2-24.6%)**
RI	18		22		21		**4 (18.2-22.2%)**	
	14	4	20	2	13	8	**4 (20-30.8%)**	**0**